

Null-field integral approach for the piezoelectricity problems with arbitrary elliptical inhomogeneities

Ying-Te Lee¹, Jeng-Tzong Chen^{1*}, Shyh-Rong Kuo¹

¹ Department of Harbor and River Engineering, National Taiwan Ocean University, Keelung 20224, Taiwan

* Corresponding author: jtchen@mail.ntou.edu.tw

Abstract Based on the successful experience of solving anti-plane problems containing arbitrary elliptical inclusions, we extend to deal with the piezoelectricity problems containing arbitrary elliptical inhomogeneities. In order to fully capture the elliptical geometry, the keypoint of the addition theorem in terms of the elliptical coordinates is utilized to expand the fundamental solution to the degenerate kernel and boundary densities are simulated by the eigenfunction expansion. Only boundary nodes are required instead of boundary elements. Therefore, the proposed approach belongs to one kind of meshless and semi-analytical methods. Besides, the error stems from the number of truncation terms of the eigenfunction expansion and the convergence rate of exponential order is better than the linear order of the conventional boundary element method. It is worth noting that there are Jacobian terms in the degenerate kernel, boundary density and contour integral. However, they would cancel each other out in the process of the boundary contour integral. As the result, the orthogonal property of eigenfunction is preserved and the boundary integral can be easily calculated. Finally, the problem of two elliptical inhomogeneities in an infinite piezoelectric material subject to anti-plane remote shear and in-plane electric field is considered to demonstrate the validity of the present method. Besides, two circular inhomogeneities can be seen as a special case to compare with the available data by approximating the major and minor axes.

Keywords Piezoelectricity, Elliptical inhomogeneity, In-plane electric field, Anti-plane shear

1. Introduction

In recent years, more and more investigators paid their attention to study the actuators and sensors because they were widely used in smart materials or structures technology. Therefore, the study of electromechanical behavior of piezoelectric material becomes an important issue. It is well-known that it results in the stress concentration when the inhomogeneities or defects exist in the materials. In this article, we extend the previous works [1] on the piezoelectricity problems with “circular” inclusions to deal with the problem containing “elliptical” inhomogeneities.

For an elliptical shape, it may be more general than a circular geometry in the practical applications. Based on the concept of complex potential, Gong and Meguid [2] used the conformal mapping and Laurent series expansion to solve an infinite medium containing an elliptical inhomogeneity under anti-plane shear. Explicit form of the stress function in the inhomogeneity as well as in the matrix was derived in their work. Then, a generalized and unified treatment was developed by Gong [3] for the elliptical inclusion embedded in an infinite matrix not only under the remote shear but also interacting by the screw dislocation. Besides, Shen *et al.* [4] developed a semi-analytical solution for the problem of an elliptical inclusion not perfectly bonded in an infinite matrix under anti-plane shear. Under the assumption of continuous tractions and discontinuous displacements across the interface, they used a model of a spring layer with thickness to simulate the interface. They found the non-uniform stress field and the average stresses in the inclusion is highly related to the aspect ratio of the inclusion and the parameter of interface simulation. For arbitrary distributed elliptical inclusions under remote shears, few works were found in literature.

To the authors' knowledge, Noda and Matsuo [5] have used the Cauchy-type singular integral equations to solve an interaction problem of elliptical inclusions distributed in an infinite medium under a longitudinal shear loading. They discussed different outlet of two elliptical inclusions as well as different ratios of shear moduli. Later, Lee and Kim [6] also revisited the problem of Noda and Matsuo by using the volume integral equation method. Lee and Chen [7] also successfully used the null-field boundary integral equation in conjunction with degenerate kernels to solve the problem. Besides, we don't find other works to discuss on this issue containing more than two inclusions.

For the piezoelectricity problems with circular inclusions, many researchers [8-12] made much contribution on this issue. However, for containing elliptical inhomogenieties, Meguid and Zhong [13] used the complex-variable method to study the problem of a piezoelectric elliptical inhomogeneity. They derived the analytical solution in their works. Pak [14] used the conformal mapping technique to obtain a closed-form solution. The previous works were very similar. The main difference is that Meguid and Zhong provided a general series solution, but Pak derived an explicit closed-form solution. Besides, numerous researchers have successfully solved similar problems with an elliptical inclusion. However, to the authors' best knowledge, we don't find any work on dealing with anti-plane piezoelectric problems containing two or more than two elliptical inclusions in the literature. This is our main concern.

In this paper, we extend the successful experience of solving piezoelectricity with circular inclusions to deal with the problem containing elliptical holes and/or inclusions. By fully employing the elliptical geometry, fundamental solutions were expanded into the degenerate kernel by using an addition theorem in terms of the elliptical coordinates, and boundary densities are approximated by the eigenfunction expansion. The proposed approach can be seen as one kind of meshless and semi-analytical methods because only collocation points on the real boundary are required and the error purely attributes to the number of truncation terms. In order to verify the accuracy for solving two or more than two elliptical inclusions, the available result of two circular-inclusion case is used to compare with the solution of present approach by numerically approaching the length of the major axis to be equal to the minor axis.

2. Problem statement and formulation

2.1. Problem statement

The problem to be considered here is an infinite piezoelectric medium with multiple elliptical inclusions under the remote anti-plane shears (σ_{zx}^∞ and σ_{zy}^∞) and the in-plane far-field electric field

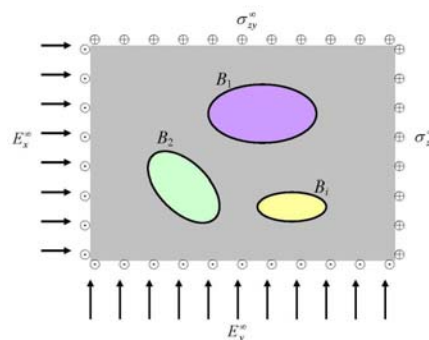


Figure 1 Sketch of the problem

(E_x^∞ and E_y^∞) as shown in Fig. 1. Bleustein [12] has pointed out that if one takes the plane normal to the poling direction as the plane of interest, only the anti-plane displacement (w) couples with the in-plane electric fields (E_x and E_y). Therefore, only the anti-plane displacement and in-plane electric field are considered in this article such as u , v and E_z are the vanishing components. In the absence of the body forces and body charges, the governing equations coupled by the displacement and electric potential can be obtained as follows:

$$c_{44}\nabla^2 w + e_{15}\nabla^2 \Phi = 0, \quad e_{15}\nabla^2 w - \varepsilon_{11}\nabla^2 \Phi = 0, \quad (1)$$

where ∇^2 is the two-dimensional Laplacian operator, c_{44} is the elastic modulus, e_{15} is the piezoelectric constant, ε_{11} is the dielectric constant, w is the anti-plane displacement and Φ is the in-plane electric potential. From Eq.(1), we can simplify the equations as

$$\nabla^2 w = 0 \quad \text{and} \quad \nabla^2 \Phi = 0. \quad (2)$$

The constitutive equations coupled between the elastic field and electric field are

$$\sigma_{zx} = c_{44}\gamma_{zx} - e_{15}E_x, \quad \sigma_{zy} = c_{44}\gamma_{zy} - e_{15}E_y, \quad (3)$$

$$D_x = e_{15}\gamma_{zx} + \varepsilon_{11}E_x, \quad D_y = e_{15}\gamma_{zy} + \varepsilon_{11}E_y, \quad (4)$$

where γ_{zx} and γ_{zy} are the anti-plane shear strains, and D_x and D_y are the in-plane electric displacements. By taking free body technique, the problem can be decomposed into two parts. One is an infinite piezoelectric medium with N elliptical holes (Fig.2(a)) and the other is only N -inclusions problem (Fig.2(b)). For the problem in Fig.2(a), it can be superimposed by two parts as shown in Fig.3(a) and Fig.3(b). Both the two parts in Figs. 2(b) and 3(b) satisfy the Laplace

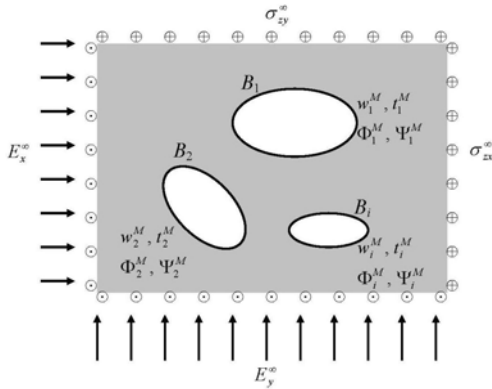


Figure 2(a) An infinite plane containing elliptical holes subject to remote shears and far-field in-plane electric fields

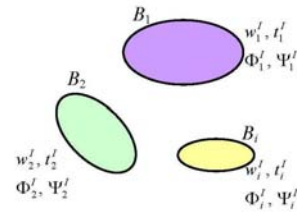


Figure 2(b) Multiple elliptical inclusions

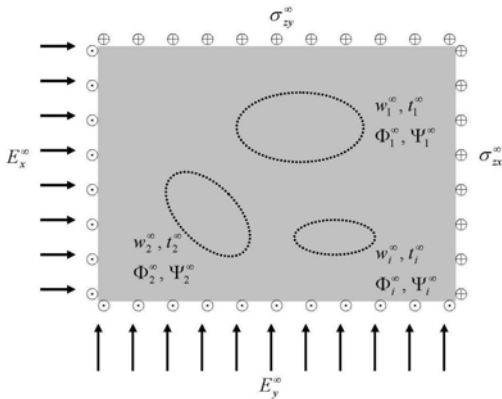


Figure 3(a) An infinite medium subject to remote shears and far-field in-plane electric fields

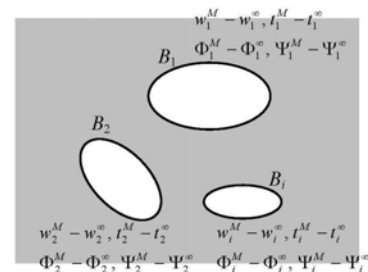


Figure 3(b) An infinite medium containing elliptical holes

equations as shown in Eq.(2). Besides, the interface between the matrix and inclusion is assumed perfectly bonded and it satisfies the following interface condition for stress fields and electric fields

$$w^M = w^I \quad \text{and} \quad \sigma_{z\xi}^M = \sigma_{z\xi}^I \quad \text{on} \quad B_k, \quad (5)$$

$$\Phi^M = \Phi^I \quad \text{and} \quad D_\xi^M = D_\xi^I \quad \text{on} \quad B_k. \quad (6)$$

2.2. Dual null-field boundary integral formulation

2.2.1 Conventional version

The integral equation for the domain point can be derived from the third Green's identity, we have

$$w(\mathbf{x}) = \int_B T(\mathbf{s}, \mathbf{x}) w(\mathbf{s}) dB(\mathbf{s}) - \int_B U(\mathbf{s}, \mathbf{x}) t(\mathbf{s}) dB(\mathbf{s}), \quad \mathbf{x} \in D, \quad (7)$$

$$t(\mathbf{x}) = \int_B M(\mathbf{s}, \mathbf{x}) w(\mathbf{s}) dB(\mathbf{s}) - \int_B L(\mathbf{s}, \mathbf{x}) t(\mathbf{s}) dB(\mathbf{s}), \quad \mathbf{x} \in D, \quad (8)$$

where B is the boundary, \mathbf{s} and \mathbf{x} are the source and field points, respectively, $t(\mathbf{x}) = \partial w(\mathbf{x}) / \partial \mathbf{n}_x$, $t(\mathbf{s}) = \partial w(\mathbf{s}) / \partial \mathbf{n}_s$, \mathbf{n}_s and \mathbf{n}_x denote the outward normal vectors at the source point \mathbf{s} and field point \mathbf{x} , respectively, D is the domain of interest and the kernel function, $U(\mathbf{s}, \mathbf{x}) = \frac{1}{2\pi} \ln r$

($r \equiv |\mathbf{x} - \mathbf{s}|$), is the fundamental solution which satisfies

$$\nabla^2 U(\mathbf{x}, \mathbf{s}) = \delta(\mathbf{x} - \mathbf{s}), \quad (9)$$

in which $\delta(\mathbf{x} - \mathbf{s})$ denotes the Dirac-delta function. The other kernel functions, $T(\mathbf{s}, \mathbf{x})$, $L(\mathbf{s}, \mathbf{x})$, and $M(\mathbf{s}, \mathbf{x})$, are defined by

$$T(\mathbf{s}, \mathbf{x}) = \frac{\partial U(\mathbf{s}, \mathbf{x})}{\partial \mathbf{n}_s}, \quad L(\mathbf{s}, \mathbf{x}) = \frac{\partial U(\mathbf{s}, \mathbf{x})}{\partial \mathbf{n}_x}, \quad M(\mathbf{s}, \mathbf{x}) = \frac{\partial^2 U(\mathbf{s}, \mathbf{x})}{\partial \mathbf{n}_s \partial \mathbf{n}_x}. \quad (10)$$

By moving the field point \mathbf{x} to the boundary, the dual boundary integral equations for the boundary point can be obtained as follows:

$$\frac{1}{2} w(\mathbf{x}) = C.P.V. \int_B T(\mathbf{s}, \mathbf{x}) w(\mathbf{s}) dB(\mathbf{s}) - \int_B U(\mathbf{s}, \mathbf{x}) t(\mathbf{s}) dB(\mathbf{s}), \quad \mathbf{x} \in B, \quad (11)$$

$$\frac{1}{2} t(\mathbf{x}) = H.P.V. \int_B M(\mathbf{s}, \mathbf{x}) w(\mathbf{s}) dB(\mathbf{s}) - C.P.V. \int_B L(\mathbf{s}, \mathbf{x}) t(\mathbf{s}) dB(\mathbf{s}), \quad \mathbf{x} \in B, \quad (12)$$

where $C.P.V.$ and $H.P.V.$ denote the Cauchy principal value and Hadamard (or called Mangler) principal value, respectively. Besides, once the field point \mathbf{x} locates outside the domain ($\mathbf{x} \in D^c$), we obtain the dual null-field integral equations as shown below

$$0 = \int_B T(\mathbf{s}, \mathbf{x}) w(\mathbf{s}) dB(\mathbf{s}) - \int_B U(\mathbf{s}, \mathbf{x}) t(\mathbf{s}) dB(\mathbf{s}), \quad \mathbf{x} \in D^c, \quad (13)$$

$$0 = \int_B M(\mathbf{s}, \mathbf{x}) w(\mathbf{s}) dB(\mathbf{s}) - \int_B L(\mathbf{s}, \mathbf{x}) t(\mathbf{s}) dB(\mathbf{s}), \quad \mathbf{x} \in D^c, \quad (14)$$

where D^c is the complementary domain. Equations (7), (8), (13) and (14) are conventional formulations where the point is not located on the real boundary. Singularity occurs and concept of principal values is required once Eqs.(11) and (12) are considered. The traction $t(\mathbf{s})$ is the directional derivative of $w(\mathbf{s})$ along the outer normal direction at \mathbf{s} . In order to satisfy the interface condition, the collocation points are located on the boundary. For calculating the stress in the domain, the normal vector of an interior point is artificially given, e.g. $t(\mathbf{x}) = \partial w(\mathbf{x}) / \partial x$, if $\mathbf{n}_x = (1, 0)$ and $t(\mathbf{x}) = \partial w(\mathbf{x}) / \partial y$, if $\mathbf{n}_x = (0, 1)$. In other words, the selection of \mathbf{n} depends on the stress under consideration.

2.2.2 Present version

By introducing the degenerate kernels, the collocation point can be located on the real

boundary free of calculating principal value using a small circular bump. Therefore, the representations of integral equations including the boundary point for the interior problem can be written as

$$w(\mathbf{x}) = \int_B T^i(\mathbf{s}, \mathbf{x})w(\mathbf{s}) dB(\mathbf{s}) - \int_B U^i(\mathbf{s}, \mathbf{x})t(\mathbf{s}) dB(\mathbf{s}), \mathbf{x} \in D \cup B, \quad (15)$$

$$t(\mathbf{x}) = \int_B M^i(\mathbf{s}, \mathbf{x})w(\mathbf{s}) dB(\mathbf{s}) - \int_B L^i(\mathbf{s}, \mathbf{x})t(\mathbf{s}) dB(\mathbf{s}), \mathbf{x} \in D \cup B, \quad (16)$$

and

$$0 = \int_B T^e(\mathbf{s}, \mathbf{x})w(\mathbf{s}) dB(\mathbf{s}) - \int_B U^e(\mathbf{s}, \mathbf{x})t(\mathbf{s}) dB(\mathbf{s}), \mathbf{x} \in D^c \cup B, \quad (17)$$

$$0 = \int_B M^e(\mathbf{s}, \mathbf{x})w(\mathbf{s}) dB(\mathbf{s}) - \int_B L^e(\mathbf{s}, \mathbf{x})t(\mathbf{s}) dB(\mathbf{s}), \mathbf{x} \in D^c \cup B, \quad (18)$$

once the kernels are expressed in terms of an appropriate degenerate forms (denoted by subscripts i and e) instead of the closed-form fundamental solution. It is noted that \mathbf{x} in Eqs.(15)-(18) can be exactly located on the real boundary.

For the exterior problem, the domain of interest (D) is in the external region of the elliptical boundary and the complementary domain (D^c) is in the internal region of the ellipse. Therefore, the null-field boundary integral equations are represented as

$$w(\mathbf{x}) = \int_B T^e(\mathbf{s}, \mathbf{x})w(\mathbf{s}) dB(\mathbf{s}) - \int_B U^e(\mathbf{s}, \mathbf{x})t(\mathbf{s}) dB(\mathbf{s}), \mathbf{x} \in D \cup B, \quad (19)$$

$$t(\mathbf{x}) = \int_B M^e(\mathbf{s}, \mathbf{x})w(\mathbf{s}) dB(\mathbf{s}) - \int_B L^e(\mathbf{s}, \mathbf{x})t(\mathbf{s}) dB(\mathbf{s}), \mathbf{x} \in D \cup B, \quad (20)$$

and

$$0 = \int_B T^i(\mathbf{s}, \mathbf{x})w(\mathbf{s}) dB(\mathbf{s}) - \int_B U^i(\mathbf{s}, \mathbf{x})t(\mathbf{s}) dB(\mathbf{s}), \mathbf{x} \in D^c \cup B, \quad (21)$$

$$0 = \int_B M^i(\mathbf{s}, \mathbf{x})w(\mathbf{s}) dB(\mathbf{s}) - \int_B L^i(\mathbf{s}, \mathbf{x})t(\mathbf{s}) dB(\mathbf{s}), \mathbf{x} \in D^c \cup B, \quad (22)$$

Also, the observation point \mathbf{x} in Eqs.(19)-(22) can be exactly located on the real boundary. For various problems (interior or exterior), we used different kernel functions (denoted by superscripts “ i ” and “ e ”) so that the jump behavior across boundary can be captured. Therefore, different expressions of the kernels for the interior and exterior observer points are used and they will be elaborated on later.

2.2.3 Expansions of the fundamental solution and the boundary density

Based on the separable property, the kernel function $U(\mathbf{s}, \mathbf{x})$ can be expanded into degenerate form by employing the separating technique for source point and field point under the elliptical coordinates. The fundamental solution, $U(\mathbf{s}, \mathbf{x})$, in terms of degenerate (separable) kernel is shown below:

$$U(\mathbf{s}, \mathbf{x}) = \begin{cases} U^i(\bar{\xi}, \bar{\eta}; \xi, \eta) = \frac{1}{2\pi} \left(\bar{\xi} + \ln \frac{c}{2} - \sum_{m=1}^{\infty} \frac{2}{m} e^{-m\bar{\xi}} \cosh m\xi \cos m\eta \cos m\bar{\eta} \right. \\ \quad \left. - \sum_{m=1}^{\infty} \frac{2}{m} e^{-m\bar{\xi}} \sinh m\xi \sin m\eta \sin m\bar{\eta} \right), & \bar{\xi} \geq \xi, \\ U^e(\bar{\xi}, \bar{\eta}; \xi, \eta) = \frac{1}{2\pi} \left(\xi + \ln \frac{c}{2} - \sum_{m=1}^{\infty} \frac{2}{m} e^{-m\bar{\xi}} \cosh m\bar{\xi} \cos m\eta \cos m\bar{\eta} \right. \\ \quad \left. - \sum_{m=1}^{\infty} \frac{2}{m} e^{-m\bar{\xi}} \sinh m\bar{\xi} \sin m\eta \sin m\bar{\eta} \right), & \bar{\xi} < \xi, \end{cases} \quad (23)$$

where the position of the source point is $\mathbf{s} = (\bar{\xi}, \bar{\eta})$ and the field point is $\mathbf{x} = (\xi, \eta)$, the superscripts “ i ” and “ e ” denote the interior ($\bar{\xi} \geq \xi$) and exterior ($\bar{\xi} < \xi$) cases, respectively. The other kernels in the boundary integral equation can be obtained by utilizing the operators of Eq.(10) with respect to the kernel $U(\mathbf{s}, \mathbf{x})$. In the real computation, the degenerate kernel can be expressed as finite sums of products of functions of \mathbf{s} alone and functions of \mathbf{x} alone.

For the k th boundary densities, we apply the eigenfunction expansions to approximate the potential $w(\mathbf{s})$ and its normal derivative $t(\mathbf{s})$ on the boundary

$$w(\mathbf{s}) = a_0 + \sum_{n=1}^{\infty} a_n \cos n\bar{\eta} + \sum_{n=1}^{\infty} b_n \sin n\bar{\eta}, \quad (24)$$

$$t(\mathbf{s}) = \frac{1}{J_s} (p_0 + \sum_{n=1}^{\infty} p_n \cos n\bar{\eta} + \sum_{n=1}^{\infty} q_n \sin n\bar{\eta}), \quad (25)$$

where a_0 , a_n , b_n , p_0 , p_n and q_n are the coefficients of the Fourier series, $\bar{\eta}$ is the angle ($0 \leq \bar{\eta} < 2\pi$) and J_s is the Jacobian with respect to the source point and the definition is

$$J_s(\bar{\xi}, \bar{\eta}) = c\sqrt{(\sinh \bar{\xi} \cos \bar{\eta})^2 + (\cosh \bar{\xi} \sin \bar{\eta})^2}. \quad (26)$$

Here, it can be observed that the terms of J_s which may exist in the degenerate kernel, boundary density and boundary integral are cancelled out each other naturally in the boundary integration. Therefore, the elliptic integral is not required to deal with. In the real computation, only the finite M number of terms is used in the summation. The present method belongs to one kind of semi-analytical methods since error only attributes to the truncation of eigenfunction expansions.

2.2.4 Linear algebraic system

In order to calculate the Fourier coefficients, N_p ($N_p=2M+1$) boundary nodes for each elliptical boundary are needed and they are uniformly collocated on each elliptical boundary. After locating the null-field point \mathbf{x}_k exactly on the k th elliptical boundary in Eq.(17), we have

$$0 = \sum_{j=1}^N \int_{B_j} T(\mathbf{s}, \mathbf{x}) w(\mathbf{s}) dB_j(\mathbf{s}) - \sum_{j=1}^N \int_{B_j} U(\mathbf{s}, \mathbf{x}) t(\mathbf{s}) dB_j(\mathbf{s}), \quad \mathbf{x} \in D^c \cup B, \quad (27)$$

where N is the number of boundary elements. Since the boundary integral equations are frame indifferent, *i.e.* objectivity rule is satisfied. The origin of observer system is adaptively chosen at the center of elliptical boundary under integration. For the B_j integral of the j th elliptical boundary, the kernels of $U(\mathbf{s}, \mathbf{x})$ and $T(\mathbf{s}, \mathbf{x})$ are expressed in terms of degenerate kernels, and $w(\mathbf{s})$ and $t(\mathbf{s})$ are substituted by using the Fourier series. For simplicity, a linear algebraic system is obtained

$$[\mathbf{U}]\{\mathbf{t}\} = [\mathbf{T}]\{\mathbf{w}\}, \quad (28)$$

where $[\mathbf{U}]$ and $[\mathbf{T}]$ are the influence matrices with a dimension of $N \times (2M + 1)$ by $N \times (2M + 1)$, $\{\mathbf{u}\}$ and $\{\mathbf{t}\}$ denote the column vectors of Fourier coefficients with a dimension of $N \times (2M + 1)$ by 1 in which $[\mathbf{U}]$, $[\mathbf{T}]$, $\{\mathbf{u}\}$ and $\{\mathbf{t}\}$ can be defined as follows:

$$[\mathbf{U}] = \begin{bmatrix} \mathbf{U}_{11} & \mathbf{U}_{12} & \cdots & \mathbf{U}_{1N} \\ \mathbf{U}_{21} & \mathbf{U}_{22} & \cdots & \mathbf{U}_{2N} \\ \vdots & \vdots & \ddots & \vdots \\ \mathbf{U}_{N1} & \mathbf{U}_{N2} & \cdots & \mathbf{U}_{NN} \end{bmatrix}, \quad [\mathbf{T}] = \begin{bmatrix} \mathbf{T}_{11} & \mathbf{T}_{12} & \cdots & \mathbf{T}_{1N} \\ \mathbf{T}_{21} & \mathbf{T}_{22} & \cdots & \mathbf{T}_{2N} \\ \vdots & \vdots & \ddots & \vdots \\ \mathbf{T}_{N1} & \mathbf{T}_{N2} & \cdots & \mathbf{T}_{NN} \end{bmatrix}, \quad \{\mathbf{w}\} = \begin{Bmatrix} \mathbf{w}_1 \\ \mathbf{w}_2 \\ \vdots \\ \mathbf{w}_N \end{Bmatrix}, \quad \{\mathbf{t}\} = \begin{Bmatrix} \mathbf{t}_1 \\ \mathbf{t}_2 \\ \vdots \\ \mathbf{t}_N \end{Bmatrix}, \quad (29)$$

where the vectors $\{\mathbf{w}_k\}$ and $\{\mathbf{t}_k\}$ are in the forms of $\{a_0^k a_1^k b_1^k \cdots a_M^k b_M^k\}^T$ and $\{p_0^k p_1^k q_1^k \cdots p_M^k q_M^k\}^T$, respectively; the first subscript “ j ” ($j=1, 2, \dots, N$) in $[\mathbf{U}_{jk}]$ and $[\mathbf{T}_{jk}]$ denotes the index of the j th ellipse where the collocation point is located and the second subscript “ k ” ($k=1, 2, \dots, N$) denotes the index of the k th ellipse where the boundary data $\{\mathbf{w}_k\}$ and $\{\mathbf{t}_k\}$ are specified and M indicates the truncated terms of eigenfunction expansions.

2.2.5 Solution procedures and interface conditions

In the real computation, two problems in Figure 2(b) and Figure 3(b) are solved by using the present formulation. For the exterior problem of the matrix in Figure 3(b), we have

$$[\mathbf{T}^M]\{\mathbf{w}^M - \mathbf{w}^\infty\} - [\mathbf{U}^M]\{\mathbf{t}^M - \mathbf{t}^\infty\} = \{\mathbf{0}\}, \quad (30)$$

$$[\mathbf{T}^M]\{\Phi^M - \Phi^\infty\} - [\mathbf{U}^M]\{\Psi^M - \Psi^\infty\} = \{\mathbf{0}\}, \quad (31)$$

from Eq.(22). For the interior problem of each inclusion in Figure 2(b), we have

$$[\mathbf{T}^I]\{\mathbf{w}^I\} - [\mathbf{U}^I]\{\mathbf{t}^I\} = \{\mathbf{0}\}, \quad (32)$$

$$[\mathbf{T}^I]\{\Phi^I\} - [\mathbf{U}^I]\{\Psi^I\} = \{\mathbf{0}\}, \quad (33)$$

from Eq.(18), where the subscripts “ M ” and “ I ” denote the matrix and inclusion, respectively. The four influence matrices, $[\mathbf{U}^M]$, $[\mathbf{T}^M]$, $[\mathbf{U}^I]$ and $[\mathbf{T}^I]$, are obtained from the degenerate kernels, while $\{\mathbf{w}^M\}$, $\{\mathbf{t}^M\}$, $\{\mathbf{w}^I\}$, $\{\mathbf{t}^I\}$, $\{\Phi^M\}$, $\{\Psi^M\}$, $\{\Phi^I\}$, $\{\Psi^I\}$ represent the coefficient vectors of eigenfunction expansions. Based on the continuity of displacement and equilibrium of traction between the interface of matrix and the k th inclusion as shown in Eqs.(6) and (7), we have

$$\{\mathbf{w}^M\} - \{\mathbf{w}^I\} = \{\mathbf{0}\}, \quad (34)$$

$$[\mathbf{c}_{44}^M]\{\mathbf{t}^M\} + [\mathbf{c}_{44}^I]\{\mathbf{t}^I\} + [\mathbf{e}_{15}^M]\{\Psi^M\} + [\mathbf{e}_{15}^I]\{\Psi^I\} = \{\mathbf{0}\}, \quad (35)$$

$$\{\Phi^M\} - \{\Phi^I\} = \{\mathbf{0}\}, \quad (36)$$

$$[\mathbf{e}_{15}^M]\{\mathbf{t}^M\} + [\mathbf{e}_{15}^I]\{\mathbf{t}^I\} - [\mathbf{\epsilon}_{11}^M]\{\Psi^M\} - [\mathbf{\epsilon}_{11}^I]\{\Psi^I\} = \{\mathbf{0}\}, \quad (37)$$

where $[\mathbf{c}_{44}^M]$, $[\mathbf{e}_{15}^M]$, $[\mathbf{\epsilon}_{11}^M]$, $[\mathbf{c}_{44}^I]$, $[\mathbf{e}_{15}^I]$ and $[\mathbf{\epsilon}_{11}^I]$ are the diagonal matrices to the material parameters. According to Eqs.(30)-(37), we have a linear system as follows:

$$\begin{bmatrix} \mathbf{T}^M & -\mathbf{U}^M & \mathbf{0} & \mathbf{0} & \mathbf{0} & \mathbf{0} & \mathbf{0} & \mathbf{0} \\ \mathbf{0} & \mathbf{0} & \mathbf{T}^I & -\mathbf{U}^I & \mathbf{0} & \mathbf{0} & \mathbf{0} & \mathbf{0} \\ \mathbf{0} & \mathbf{0} & \mathbf{0} & \mathbf{0} & \mathbf{T}^M & -\mathbf{U}^M & \mathbf{0} & \mathbf{0} \\ \mathbf{0} & \mathbf{0} & \mathbf{0} & \mathbf{0} & \mathbf{0} & \mathbf{0} & \mathbf{T}^I & -\mathbf{U}^I \\ \mathbf{I} & \mathbf{0} & -\mathbf{I} & \mathbf{0} & \mathbf{0} & \mathbf{0} & \mathbf{0} & \mathbf{0} \\ \mathbf{0} & \mathbf{c}_{44}^M & \mathbf{0} & \mathbf{c}_{44}^I & \mathbf{0} & \mathbf{e}_{15}^M & \mathbf{0} & \mathbf{e}_{15}^I \\ \mathbf{0} & \mathbf{0} & \mathbf{0} & \mathbf{0} & \mathbf{I} & \mathbf{0} & -\mathbf{I} & \mathbf{0} \\ \mathbf{0} & \mathbf{e}_{15}^M & \mathbf{0} & \mathbf{e}_{15}^I & \mathbf{0} & -\mathbf{\epsilon}_{11}^M & \mathbf{0} & -\mathbf{\epsilon}_{11}^I \end{bmatrix} \begin{bmatrix} \mathbf{w}^M \\ \mathbf{t}^M \\ \mathbf{w}^I \\ \mathbf{t}^I \\ \Phi^M \\ \Psi^M \\ \Phi^I \\ \Psi^I \end{bmatrix} = \begin{bmatrix} \mathbf{a} \\ \mathbf{0} \\ \mathbf{b} \\ \mathbf{0} \\ \mathbf{0} \\ \mathbf{0} \\ \mathbf{0} \\ \mathbf{0} \end{bmatrix}, \quad (38)$$

where $[\mathbf{I}]$ is the identity matrix and $\{\mathbf{a}\}$ and $\{\mathbf{b}\}$ are the forcing terms due to the remote shear stress as shown below

$$\{\mathbf{a}\} = [\mathbf{T}^M]\{\mathbf{w}^\infty\} - [\mathbf{U}^M]\{\mathbf{t}^\infty\}, \quad (39)$$

$$\{\mathbf{b}\} = [\mathbf{T}^M]\{\Phi^\infty\} - [\mathbf{U}^M]\{\Psi^\infty\}. \quad (40)$$

From Eq. (38), the unknown Fourier coefficients can be easily determined.

3. Numerical examples and discussions

To the authors’ knowledge, we don’t find any paper to discuss on the piezoelectricity with two or more than two elliptical inhomogeneities. Therefore, we consider the available case containing two circular inhomogeneities to demonstrate the validity of present approach for dealing with a problem containing two elliptical inhomogeneities. Besides, we also provide a numerical example for the case containing two elliptical inhomogeneities.

Case1: An infinite medium with two circular inhomogeneities

The first example considered here is an infinite medium with two elliptical inhomogeneities. Here, we used the limiting concept by numerically setting the semi-major and semi-minor axes to be near the same by using 1.000000 and 0.999999 for the first inclusion and 2.000000 and 1.999999 for the second inclusion to compare with the available results of two circular inclusions subject to remote shears and electric fields. The mechanical and electric parameters of medium and inhomogeneities are

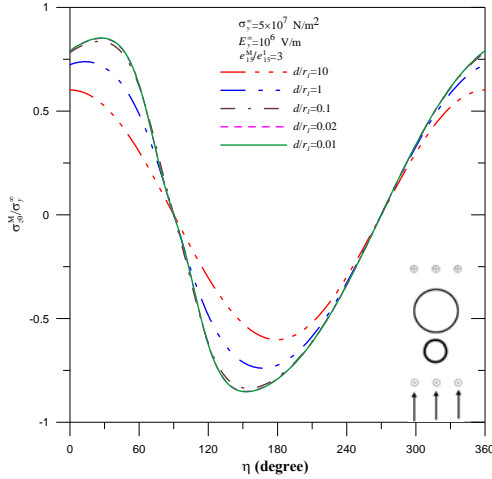


Figure 4(a) Tangential stress distribution for different ratios d/r_1 with $e_{15}^M/e_{15}^I = 3$

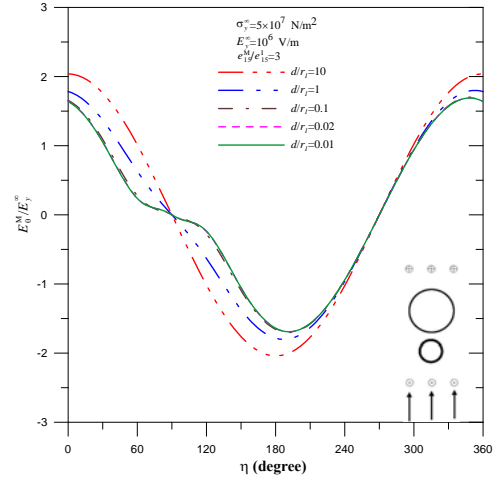


Figure 4(b) Tangential electric field distribution for different ratios d/r_1 with $e_{15}^M/e_{15}^I = 3$

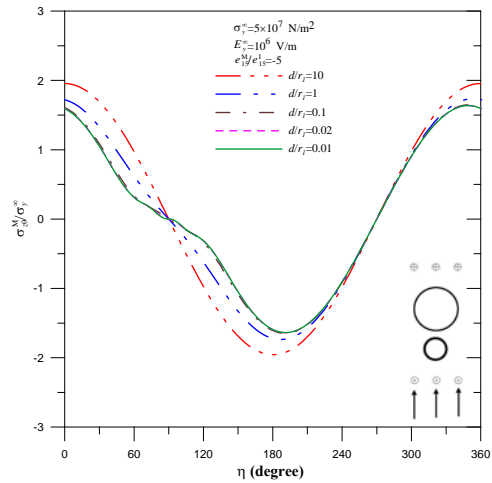


Figure 5(a) Tangential stress distribution for different ratios d/r_1 with $e_{15}^M/e_{15}^I = -5$

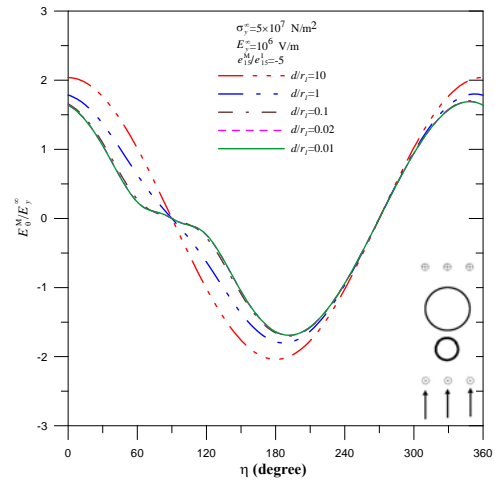


Figure 5(b) Tangential electric field distribution for different ratios d/r_1 with $e_{15}^M/e_{15}^I = -5$

given as $c_{44}^M = c_{44}^I = 3.53 \times 10^{10} \text{ N/m}^2$, $\varepsilon_{44}^M = \varepsilon_{44}^I = 1.51 \times 10^{-8} \text{ C/Vm}$, $e_{15}^I = 10 \text{ C/m}^2$. The remote shears are

$\sigma_{zx}^\infty = 0$, $\sigma_{zy}^\infty = 5 \times 10^7 \text{ N/m}^2$ and far-field electric fields are given as $E_x^\infty = 0$ and $E_y^\infty = 10^6 \text{ V/m}$. All

the numerical results are given below by using the 30 terms of eigenfunction (M). In order to examine the generality of the present formulation for the problem containing two elliptical inclusions, the case of an infinite medium with the two circular inclusions ($r_2 = 2r_1$) paralleled to the applied loadings ($\beta = 90^\circ$) is used to verify the present approach. Figures 4(a) and 4(b), respectively, show the tangential shear stress and tangential electric field distribution in the matrix

along the boundary of the smaller inhomogeneity for the ratio of $e_{15}^M/e_{15}^I = 3$. After comparing with

the results of Chao and Chang [10] and Chen and Wu [1], it can be found that good agreement is made. By changing the ratio of the piezoelectric constant, Figures 5(a) and 5(b), respectively, show

the tangential stress and tangential electric field distribution corresponding to $e_{15}^M/e_{15}^I = -5$. The two figures also show the consistency between the present data and those of Chen and Wu [1].

However,

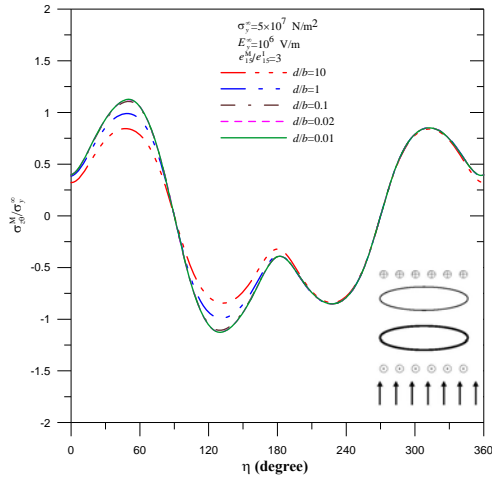


Figure 6(a) Tangential stress distribution for different ratios d/b with $e_{15}^M/e_{15}^I = 3$

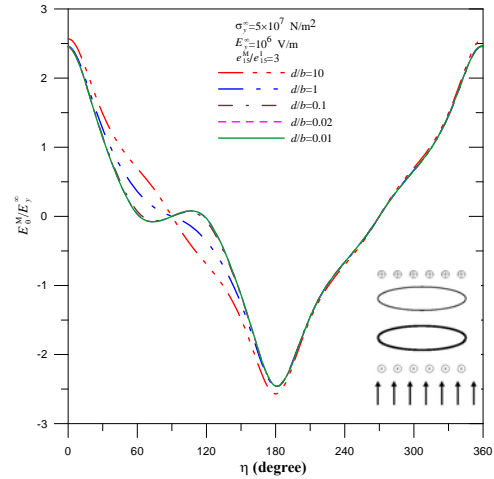


Figure 6(b) Tangential electric field distribution for different ratios d/b with $e_{15}^M/e_{15}^I = 3$

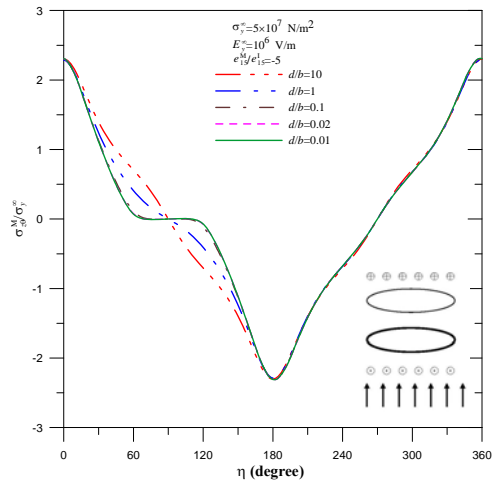


Figure 7(a) Tangential stress distribution for different ratios d/b with $e_{15}^M/e_{15}^I = -5$

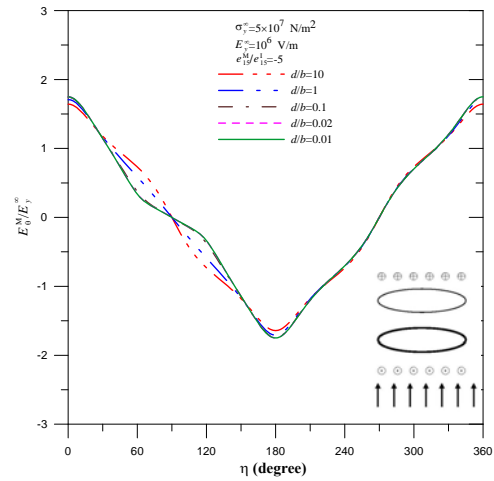


Figure 7(b) Tangential electric field distribution for different ratios d/b with $e_{15}^M/e_{15}^I = -5$

in the Chao and Chang's paper [10], it changes very sharply near $\theta = 90^\circ$ and is not consistent with our results when two inclusions are very close to each other ($d/r_1 = 0.01$ and 0.02). It is open for discussions why our results are different from those of Chao and Chang near $\theta = 90^\circ$.

Case2: An infinite medium with two elliptical inhomogeneities

In this case, the two elliptical inhomogeneities arrayed paralleled to the applied loadings ($\beta = 90^\circ$) are considered. The semi-major (a) and semi-minor (b) axes are 2 and 1 for two inhomogeneities. The tangential stress and tangential electric field in the matrix along the boundary of the lower inhomogeneity for different ratios of d/b are plotted in Figures 6(a) and 6(b), respectively. For the different ratio of the piezoelectric constant ($e_{15}^M/e_{15}^I = -5$), the tangential stress and tangential electric field in the matrix along the lower inhomogeneity are given in Figures 7(a) and 7(b), respectively. It can be found that the stress concentration in the case of containing the elliptical inhomogeneities is greater than the case of containing circular ones. Since there are few literatures for discussions on the piezoelectricity containing two elliptical inhomogeneities, we used the limiting case as given in Case 1 to verify the validity of our program. Further, we provided a

case containing two identical elliptical inhomogenities and it can be a benchmark for comparison when other numerical method is developed.

4. Conclusion

We have successfully proposed a systematic method to solve an infinite plane containing elliptical inclusions under remote anti-plane shears and in-plane electric fields. Although a Jacobian term may appear in the degenerate kernel, boundary density and boundary contour integral by using the elliptical coordinates, it can be cancelled out in our formulation to preserve the orthogonal condition. Although the work containing two elliptical inhomogenities is not available in the literature, the piezoelectricity with two circular inclusions is used as a limiting case to demonstrate the validity of present approach. Besides, the case containing two identical elliptical inhomogenities was provided as a benchmark example. The developed program can be generally used for piezoelectricity problems containing elliptical inhomogenities of arbitrary number, position, size and inclination angle.

Acknowledgements

This research was partially supported by the National Science Council in Taiwan through Grant NSC 101-2811-E-019-002.

References

- [1] J.T. Chen, A.C. Wu, Null-field approach for piezoelectricity problems with arbitrary circular inclusions," *Eng Anal Bound Elem*, 30 (2006) 971-993.
- [2] S.X. Gong, S.A. Meguid, A general treatment of the elastic field of an elliptical inhomogeneity under antiplane shear. *J Appl Mech-ASME*, 59 (1992) 131-135.
- [3] S.X. Gong, A unified treatment of the elastic elliptical inhomogeneity under antiplane shear, *Arch Appl Mech*, 65 (1995) 55-64.
- [4] H. Shen, P. Schiavone, C.Q. Ru, A. Mioduchowski, An elliptic inclusion with imperfect interface in anti-plane shear," *Int J Solids Struct*, 37 (2000) 4557-4575.
- [5] N.A. Noda, T. Matsuo, Stress analysis of arbitrarily distributed elliptical inclusions under longitudinal shear loading. *Int J Fract*, 106 (2000) 81-93.
- [6] J. Lee, H.R. Kim, Volume integral equation method for multiple circular and elliptical inclusion problems in antiplane elastostatics. *Composites Part: B*, 43 (2012) 1224-1243.
- [7] Y.T. Lee, J.T. Chen, Null-field approach for the antiplane problem with elliptical holes and/or inclusions. *Composites Part: B*, 44 (2013) 283-294.
- [8] Y.E. Pak, Circular inclusion problem in antiplane piezoelectricity. *Int J Solids Struct*, 29 (1996) 2403-2419.
- [9] T. Honein, B.V. Honein, E. Honein, G. Herrmann, On the interaction of two piezoelectric fibers embedded in an intelligent material. *J Intell Mater Syst Struct*, 6 (1995) 229-236.
- [10] C.K. Chao, K.J. Chang, Interacting circular inclusions in antiplane piezoelectricity. *Int J Solids Struct*, 36 (1999) 3349-3373.
- [11] X. Wang, Y.P. Shen, On double circular inclusion problem in antiplane piezoelectricity. *Int J Solids Struct*, 38 (2001) 4439-4461.
- [12] J.L. Bleustein, New surface wave in piezoelectric materials, *Appl Phys Lett*, 46 (1968) 412-413.
- [13] S.A. Meguid, Z. Zhong, Electroelastic analysis of a piezoelectric elliptical inhomogeneity. *Int J Solids Struct*, 34, pp. 3401-3414, 1997.
- [14] Y.E. Pak, Elliptical inclusion problem in antiplane piezoelectricity: implications for fracture mechanics. *Int. J. Solids Struct.*, Vol. 48 pp. 209-222, 2010.